Title

CLOSURE MECHANISMS FOR THE INFLUENCE OF LOAD RATIO ON FATIGUE CRACK PROPAGATION IN STEELS

Authors

Suresh, S.
Ritchie, R.O.

Publication Date

1982-04-01

LBL-14280
Preprint

Lawrence Berkeley Laboratory
UNIVERSITY OF CALIFORNIA

Materials & Molecular Research Division

Submitted to Acta Metallurgica

CLOSURE MECHANISMS FOR THE INFLUENCE OF LOAD RATIO ON FATIGUE CRACK PROPAGATION IN STEELS

S. Suresh and R.O. Ritchie

April 1982

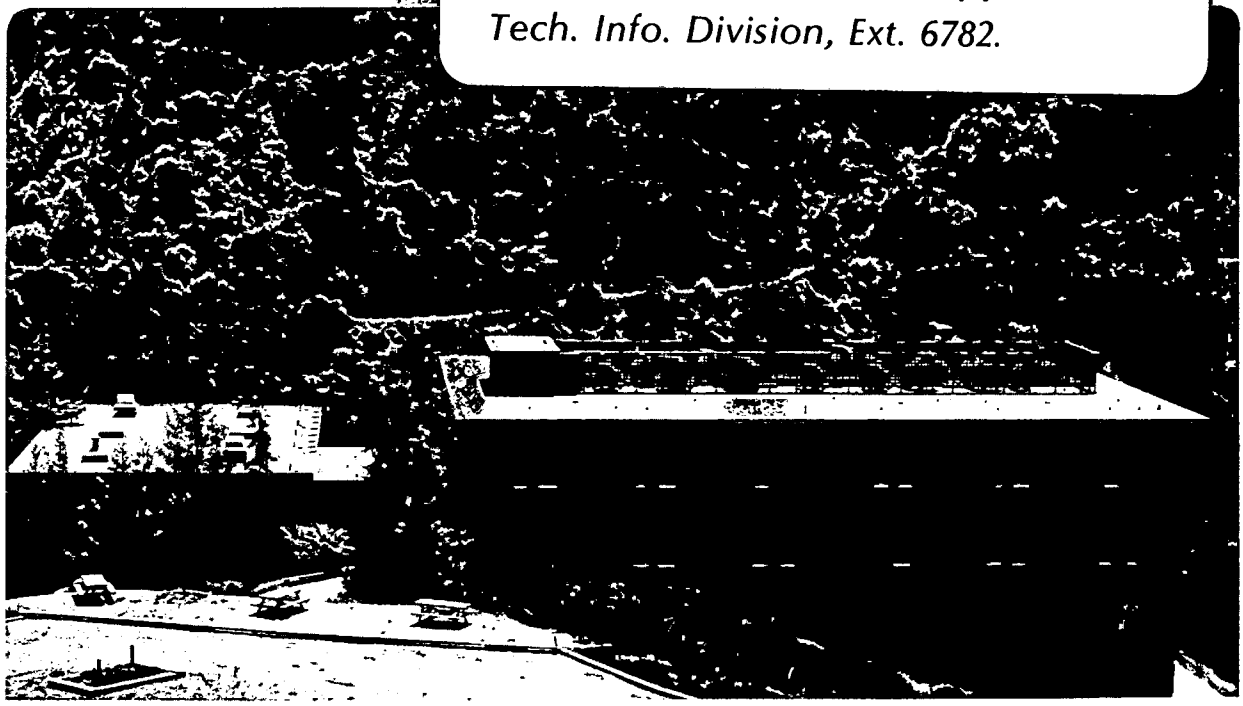

Prepared for the U.S. Department of Energy under Contract DE-AC03-76SF00098

DISCLAIMER

LBL - 14280

CLOSURE MECHANISMS FOR THE INFLUENCE OF LOAD RATIO ON FATIGUE CRACK PROPAGATION IN STEELS

By

S. Suresh and R. O. Ritchie

Materials and Molecular Research Division, Lawrence Berkeley Laboratory
and Department of Materials Science and Mineral Engineering
University of California, Berkeley, CA 94720 (U.S.A.)

April 1982

Submitted to Acta Metallurgica

This work was supported by the Director, Office of Energy Research, Office of Basic Energy Sciences, Materials Science Division of the U. S. Department of Energy under Contract No. DE-AC03-76SF00098.

CLOSURE MECHANISMS FOR THE INFLUENCE OF LOAD RATIO ON FATIGUE CRACK PROPAGATION IN STEELS

S. Suresh and R. O. Ritchie

Materials and Molecular Research Division, Lawrence Berkeley Laboratory
and Department of Materials Science and Mineral Engineering
University of California, Berkeley, CA 94720, U.S.A.

ABSTRACT - A study has been made of the influence of load ratio R on fatigue crack propagation behavior and on the value of the fatigue crack growth threshold, ΔK_0, in a bainitic 2-1/4Cr-1Mo pressure vessel steel tested in aqueous and moist and dry gaseous environments. It is found that for moist air and dry hydrogen atmospheres, threshold ΔK_0 values decrease sharply with increasing R, whereas for distilled water environments the dependence of ΔK_0 on R is far less marked. Furthermore, in the former two environments, the threshold condition is characterized by a constant maximum stress intensity at low load ratios, and a constant alternating stress intensity at high load ratios. Based on extensive measurements of crack face oxidation products using scanning Auger spectroscopy and on crack closure measurements using ultrasonics techniques, the role of load ratio in influencing near-threshold fatigue behavior is ascribed to various mechanisms of crack closure. In addition to the well-known plasticity-induced closure, simple models are described for contributions to closure arising from crack face oxide debris and from fracture surface roughness, which are specific to the ultra-low fatigue crack growth rate regime. The implications of such plasticity-induced, oxide-induced and roughness-induced closure models to the load ratio-dependence of near-threshold fatigue behavior in various environments are discussed in detail.

I. INTRODUCTION

Over the past twenty years, numerous mechanical, microstructural and environmental factors have been identified which markedly influence the behavior of fatigue cracks in engineering materials (see, for example, Ref. 1). Of these factors, the mean stress, characterized by the so-called load or stress ratio R (defined as the ratio of minimum to maximum stress) has been found to be of particular importance, since in many engineering applications, cyclic stresses are superimposed on "nominally-steady" operating stresses. Further, because many structures contain residual stresses, a mean stress may still be present even though the applied loading may be purely cyclic.

In the fracture mechanics characterization of the *propagation* of fatigue cracks, the effect of mean stress is generally considered in terms of the load ratio defined as the ratio of the minimum to maximum stress intensity in the cycle ($R = K_{min}/K_{max}$). In this context, it has been found that load ratio effects are especially relevant at ultralow crack propagation rates ($\lesssim 10^{-6}$ mm/cycle) approaching the threshold stress intensity range ΔK_o (below which cracks remain dormant or grow at experimentally undetectable rates), since the high frequency, low amplitude vibrations, which lead to such crack growth in service, often occur in the presence of larger mean operating stresses [1].

Over the past ten years or so, numerous investigations have sought to characterize the influence of load ratio on fatigue crack growth and on the threshold for such growth (see, for example, Ref. 1-27), although in very few instances have the mechanisms for this load ratio dependence been identified. For example, at high growth rates ($\gtrsim 10^{-4}$ mm/cycle) where the maximum stress intensity K_{max} approaches final failure or instability (characterized by the fracture toughness K_c or limit load), the marked increase in growth rates observed with increasing load ratio has been attributed to the presence of "brittle" fracture mechanisms [8,9]. These

so-called "static modes" [8], namely transgranular and intergranular cleavage and microvoid coalescence, occur in addition to, or in place of, the normal ductile striation mechanism of crack advance. Since such static modes are primarily stress (or hydrostatic stress) controlled, the resulting crack propagation rates are strongly dependent upon K_{max}, and hence dependent upon the value of the load ratio (as $K_{max} = \Delta K/(1-R)$). At intermediate growth rates (typically $\sim 10^{-6}$ to 10^{-4} mm/cycle), however, crack growth behavior becomes primarily load ratio-independent, at least in steels where environmental effects are minimal [22]. But as growth rates are reduced below $\sim 10^{-6}$ mm/cycle into the near-threshold regime, a marked influence of load ratio on fatigue behavior again becomes apparent [10].

To date, the load ratio-dependence of such near-threshold crack growth (and the value of the threshold ΔK_o) has been well-documented for a number of engineering materials [1-7,10-26] although mechanistic interpretations for the effects are still lacking. Early suggestions were based on observations of an increased proportion of intergranular facets at near-threshold levels, but subsequent detailed fractographic studies have failed to find any global dependence of the extent of intergranularity on K_{max} or R [14,18,21]. More recently, explanations for the effect of load ratio on near-threshold behavior have centered around the phenomenon of crack closure, first identified by Elber [2] in aluminum alloys at much higher stress intensities. In terms of the Elber model, crack closure, or more correctly *plasticity-induced crack closure* [2,12,23-25], can be considered to arise from the fact that during fatigue crack growth, material is plastically strained at the crack tip and due to the constraint of surrounding elastic material on this residual stretch, some contact between the crack surfaces will occur at positive loads during the fatigue cycle. Since the crack is unable to propagate whilst it remains closed, the net effect of closure is to reduce the nominal ΔK values (computed from applied loads and crack length measurements) to some lower

effective value (ΔK_{eff}) actually experienced at the crack tip, i.e., $\Delta K_{eff} = K_{max} - K_{cl}$, where K_{cl} is the stress intensity at closure ($\geq K_{min}$). This concept has proven to be extremely useful in explaining, at least qualitatively, many aspects of fatigue crack propagation and has been directly applied to justify observations of mean stress-sensitive crack growth [2]. Since, as the load ratio or mean stress is raised, the crack can be considered to remain open for a larger proportion of the cycle, it follows that, at a fixed nominal ΔK, a higher R value results in a higher ΔK_{eff}. However, once the minimum stress intensity K_{min} exceeds K_{cl}, the crack remains open during the entire cycle, such that above a critical load ratio, termed R_{cr}, closure effects become insignificant, and $\Delta K_{eff} = \Delta K$ [12].

While this concept of plasticity-induced crack closure may provide a satisfactory explanation for the role of load ratio in influencing fatigue crack propagation at intermediate growth rates, its application to behavior at near-threshold levels, where load ratio effects are much larger, is at first glance questionable [1]. This follows from experimental observations which show plasticity-induced closure to be most prevalent under plane stress conditions [27], whereas near-threshold conditions are invariably associated with plane strain. Very recently, however, additional mechanisms of crack closure have been identified, based on the role of crack face corrosion deposits [23-26,28-31] and fracture surface morphology [25,33-38], which are specific to near-threshold (plane strain) conditions. It is the objective of the present paper to examine mechanisms for the influence of load ratio on fatigue thresholds and fatigue crack propagation in light of these closure concepts, and to investigate the microstructural and particularly the environmental conditions under which this load ratio-dependence is most prevalent.

II. EXPERIMENTAL PROCEDURES

The material investigated was a 2-1/4Cr-1Mo pressure vessel steel, conforming to the ASTM A542 Class 3 designation (hereafter referred to as SA542-3). The steel, of composition shown in Table I, was supplied as 175 mm thick plate and after water quenching from 954°C and tempering (7 hr) at 663°C , the microstructure was found to be fully bainitic (<3 pct ferrite), uniformly through the thickness. Ambient temperature mechanical properties are listed in Table II.

Fatigue crack propagation experiments were performed with 12.7 mm thick compact specimens (T-L orientation) on 50kN Instron electro-servo-hydraulic testing machines, operating under closed loop control at 50 Hz (sine wave). Load ratios were varied between 0.05 and 0.75. Near-threshold growth rates were determined under decreasing stress intensity (load shedding) conditions with crack lengths continuously monitored using d.c. electrical potential techniques. Threshold ΔK_o values were defined in terms of the stress intensity range to give a maximum growth rate of 10^{-8} mm/cycle [1]. Tests were performed in ambient temperature environments of moist air (30 pct relative humidity), dehumidified gaseous hydrogen (138 kPa pressure), and distilled water. Gaseous atmospheres were contained within an O-ring sealed chamber, locally clamped onto the test piece, where gas purity and dehumidification was obtained by means of an extensive purification system involving molecular sieves, cold traps and heat-bakeable stainless steel lines. Full details of such experimental procedures can be found elsewhere [1, 26, 39].

Characterization of crack surface corrosion deposits was achieved with X-ray Photoelectron(ESCA) and scanning Auger Spectroscopy using procedures outlined in Refs. 25 and 26. Scanning electron microscopy was utilized for examination of fracture surface morphologies. Direct experimental assessment of crack closure was performed using ultrasonic techniques [26,40]. Near-threshold cracks were grown in compact specimens by load-shedding in the normal manner to yield similar

crack lengths for moist air and dry hydrogen environments. Ultrasonic waves with a frequency of 2 MHz were transmitted at one edge of the specimen and received at the opposite end while the specimen was mounted on the testing machine (Fig. 1). The amplitude of the signal transmitted to the specimen was maintained at a constant value and the output from the receiver transducer was monitored with an oscilloscope. The extent of crack opening and closing was then assessed in terms of the magnitude of the transmitted signal at the receiver transducer, as the specimen was slowly loaded through a complete fatigue cycle at ΔK_o.

III. INFLUENCE OF LOAD RATIO ON THRESHOLD ΔK_o

III.1 Fatigue Crack Propagation and Threshold Results

The influence of load ratio from R = 0.05 to 0.75 on fatigue crack propagation rates (da/dN) as a function of the stress intensity range (ΔK) in SA542-3 steel is shown in Fig. 2 for testing conditions of room temperature moist air (30 pct relative humidity) with a cyclic frequency of 50 Hz. It is seen that above $\sim 10^{-5}$ mm/cycle, growth rates are insensitive to load ratio, whereas at near-threshold levels ($\lesssim 10^{-6}$ mm/cycle) growth rates are markedly increased, and threshold ΔK_o values markedly decreased, with increasing R. However, the latter observation is only apparent up to a critical load ratio of $R \approx 0.6$, beyond which near-threshold growth rates and ΔK_o values are found to be similar. The influence of environment on this behavior is illustrated in Fig. 3, where data for low strength steel tested at high frequencies (50 Hz) in wet (moist air and wet hydrogen) and dry (dehumidified hydrogen gas) atmospheres are plotted for both low and high load ratios. It can be seen that moist environments result in lower near-threshold crack growth rates and apparently higher thresholds, compared to dry environments, at low load ratios only. At high load ratios, near-threshold behavior (in both environments) is virtually identical, although subsequent studies [41] have shown

rates to be marginally higher in the moist atmospheres. Also shown in Fig. 3 is the crack propagation behavior of SA542-3 for the more corrosive environment of distilled water. The threshold stress intensity range ΔK_0 in water is higher than in moist and dry gaseous media *at all load ratios*, and in particular this difference is now most pronounced at high load ratios.

Fractographically, little difference was observed between near-threshold fracture surfaces for all environments at both low and high load ratios. A fine-scale transgranular fracture mode was seen with evidence of intergranular facets ($\lesssim$10%). However, macroscopically, near-threshold fracture surfaces were characterized by varying degrees of crack face oxide formation, identified using ESCA to be predominantly Fe_2O_3 [26]. Using Ar^+ sputtering analysis with Auger spectroscopy, the variation of the thickness of this crack face oxidation debris* was determined for SA542-3 steel tested in dry hydrogen, moist air and distilled water, and is shown in Fig. 4 as a function of both crack length (a) and crack propagation rate (da/dN). As reported previously at low load ratios [25], the oxide film thickness in moist air and dry gaseous media increases with decreasing growth rates to a peak value near the threshold some 20-40 times thicker than at high growth rates, although the extent of oxidation is considerably less in the dry environment. Oxide thicknesses measured at high load ratios in moist air and dry hydrogen show no such build up at near-threshold levels and are comparable with the limiting thickness of oxide scales formed naturally on microstructurally-polished samples freshly exposed to the same environment for similar time periods. However, the extent of crack face oxidation in distilled water is uniformly high, and comparable to the limiting thickness of naturally-formed oxide for this environment. Optical macrographs of near-threshold fracture surfaces for moist air at R = 0.05 and 0.75 and distilled water at R = 0.75 are shown in Fig.5. These indicate a

*Since one cc of Fe oxidizes to roughly 2 cc of iron oxide, these thickness measurements represent approximately the total excess material inside the crack, assuming only thickness-direction growth [26].

distinct zone of oxidation (at ΔK_o) in air at low load ratios, the absence of appreciable (visible) oxidation in air at high load ratios, and the more copious and uniform extent of oxidation in water. Thus, unlike low load ratio behavior in air and hydrogen, the crack face oxide thickness in the more oxidizing distilled water shows no tendency to decrease at high growth rates or at high load ratios. A comparison between the peak oxide thickness d_o measured on the fracture surface close to ΔK_o and the limiting naturally-occurring oxide thickness (i.e. formed on polished samples in the absence of fatigue) for the three room temperature environments is shown in Table III.

The relationship between such oxide measurements and the load ratio-dependent threshold behavior for moist air, dry hydrogen and distilled water environments is summarized in Fig.6, where the alternating and maximum stress intensities at the threshold, ΔK_o and $K_{o,max}$ respectively, are plotted as a function of R, together with the corresponding peak excess oxide thickness (d_o). It is apparent that threshold behavior in moist air and dry hydrogen is characterized by a ΔK_o decreasing with R (constant $K_{o,max}$) at low load ratios, and a ΔK_o constant with R (increasing $K_{o,max}$) at high load ratios, similar to threshold results presented previously for other low strength steels [12,23] and aluminum alloys [12]. The critical load ratio value R_{cr} separating these two modes of behavior, however, is smaller for dry hydrogen environments. Behavior in distilled water, on the other hand, is distinctly different with the dependence of threshold ΔK_o values on load ratio being considerably less marked. Similar results have been seen in rotor steels tested in water and steam environments [42]. In general terms, such load ratio-dependent threshold data in all three environments appear to be related to the extent of crack face oxidation products. By comparing the dependence of both ΔK_o and d_o on R shown in Fig.6, it is apparent that where the oxide thickness remains roughly constant with increasing R (i.e., for distilled water) the threshold stress

intensity range ΔK_o does not decrease significantly with increasing load ratios. However, for the less aggressive environments of moist air and dry hydrogen where crack face oxide debris build-up (in excess of the naturally-occurring oxide thickness) is only apparent at low load ratios, the threshold ΔK_o is observed to decrease markedly with increasing R.

III.2 Experimental Measurement of Crack Closure

A limited number of measurements were performed on the magnitude of the crack closure effect at low and high load ratios in moist air and dry hydrogen using the ultrasonic system shown in Fig. 1. Using samples fatigued to threshold levels at R = 0.05 and R = 0.50, the variation in transmitted output signal was monitored as a function of load (i.e. stress intensity) while samples were slowly loaded through complete fatigue cycles at ΔK_o. Crack opening can be inferred by a decrease in receiver signal as less of the input ultrasonic wave is transmitted across the specimen (Fig. 7). It is apparent that no immediate steep decrease is seen in receiver output with increase in load, implying that cracks do not open immediately on application of a load, but do so in a rather gradual fashion. This is consistent with the observations of Bachmann and Munz [43] that crack surfaces can remain in contact locally, while globally the crack is considered to be open. By considering the deviations in initial linearity of the curves in Fig. 7a, one can roughly estimate the stress intensities when the cracks first open. This suggests K_{cl} values of the order of 4 MPa$\sqrt{m}$ in air and 2 MPa$\sqrt{m}$ in hydrogen at R = 0.05, and <1 MPa$\sqrt{m}$ for air at R = 0.50. However, it must be emphasized that because of the inherent gradual nature of the crack opening and closing, precise definition and determination of any stress intensity associated with closure is clearly not feasible. Nevertheless, it is clear that cracks open at distinctly lower stress intensities close to ΔK_o in dry hydrogen compared to moist air at R = 0.05, and at even lower stress intensities at higher R values.

To check the validity of these conclusions, two additional experiments were conducted. When a specimen containing no fatigue crack was tested, there was no variation in the receiver signal while the applied loads were increased from zero to threshold levels (Fig. 7). Conversely, when a sample was tested with a saw cut of a length equal to the fatigue cracks, no change in receiver signal was again seen, but the output level was now similar to the fatigue cracked samples at maximum load (i.e. with cracks fully open). Such results are a strong indication of the significance of fatigue crack closure at near-threshold levels, and moreover are an indication that such closure is strongly influenced by load ratio and environment.

IV. MECHANISMS FOR LOAD RATIO DEPENDENCE

The experimental growth rate data (Figs. 2 and 3) determined in this investigation clearly confirm that, in lower strength steels, the role of load ratio in influencing fatigue crack propagation behavior, whilst being relatively insignificant at intermediate growth rates (~10^{-6} - 10^{-4} mm/cycle), is of major importance at near-threshold levels below 10^{-6} mm/cycle. Not only are near-threshold growth rates markedly increased with increasing load ratio, but values of the threshold stress intensity range ΔK_o are decreased in a manner dependent upon the nature of the environment (Fig. 6). Furthermore, the morphology of the fatigue fracture surfaces, with the exception of the extent of crack face oxidation, does not appear to be radically changed, despite the large differences in growth rates observed (Figs. 2 and 3). Such results are in general accord with previous studies on the nature of the load ratio effect at ultralow fatigue crack growth rates (for example, see Ref.1) although, as mentioned above, mechanistic explanations for this effect have not been fully documented. It is our contention that the primary origin of the influence of load

ratio on near-threshold growth rates and on the threshold ΔK_o is associated with crack closure phenomena, although the nature of these mechanisms are not confined solely to Elber-type [2] plasticity-induced closure. We now examine the various mechanisms of closure in turn.

IV. 1 Plasticity-Induced Crack Closure (PICC)

As described above, plasticity-induced closure is considered to arise from the elastic constraint in the wake of the crack tip on material elements plastically-stretched at the tip, leading to an interference between mating crack surfaces [2]. Based on experimental compliance measurements [2] and finite-element analyses [44], several authors [2,45] have proposed *empirical* models to explain the load ratio effect on fatigue crack growth in terms of the relationship between the ratio of the closure stress intensity to maximum stress intensity (K_{cl}/K_{max}) and R, namely:

$$\frac{K_{cl}}{K_{max}} = 0.5 + 0.1R + 0.4R^2 \ , \qquad (1)$$

after Elber [2], and the modified equation of Schijve [45], viz:

$$\frac{K_{cl}}{K_{max}} = 0.45 + 0.2R + 0.25R^2 + 0.1R^3 \ . \qquad (2)$$

It should be emphasized, however, that such relationships strictly pertain to crack growth at higher stress intensities where deformation conditions approach that of plane stress. Under such circumstances, a detailed, physically-based, analysis of plasticity-induced closure has been presented [46], although no such solutions for plane strain have been successfully proposed. Despite the lack

of analyses for plane strain, Paris and Schmidt [12] utilized similar concepts to explain the dependence of fatigue thresholds on load ratio, as shown in Fig. 8. On the assumption that the stress intensity associated with closure, K_{cl}, is independent of R*, and that a constant *effective* threshold stress intensity range ΔK_{th} exists (above K_{cl}) necessary to produce crack growth, the variation in measured thresholds ΔK_o (from applied loads and crack length data) with load ratio R should show two distinct regions (Fig. 8). At low load ratios, where $K_{min} \leq K_{cl}$, the maximum stress intensity at the threshold ($K_{o,max}$) appears constant, since

$$K_{o,max} = K_{cl} + \Delta K_{th}, \quad K_{min} \leq K_{cl}, \tag{3}$$

whereas at high load ratios, where $K_{min} \geq K_{cl}$, the alternating stress intensity (ΔK_o) appears constant, since

$$\Delta K_o = \Delta K_{th}, \quad K_{min} \geq K_{cl}. \tag{4}$$

Furthermore, it follows from such arguments that a critical load ratio R_{cr} should exist, above which closure effects are unimportant. In the above analysis, this corresponds to the value of the load ratio where $K_{o,max}$ is no longer constant with R, i.e. where $K_{min} = K_{cl}$, such that

$$R = R_{cr}, \text{ when } K_{min} = K_{cl}, \text{ such that } \Delta K_{th} = \Delta K_o. \tag{5}$$

Although such closure, as defined by Elber [2], arises from interference

---

*This assumption incidently is contrary to the results of the plane stress analysis of Budiansky and Hutchinson [46] where K_{cl} is predicted to increase with R.

between crack surfaces *in the wake of the crack tip* due to the residual stretch of material elements previously plastically-strained at the tip, it is possible to effectively model this phenomenon, and to estimate values of R_{cr}, by considering the influence of the residual compressive stress field on unloading to the minimum stress intensity [47]. Following Rice's solutions for cyclic crack extension in an elastic-perfectly plastic solid [48], such stresses (σ_r) exist over a distance *ahead* of the crack tip comparable with the cyclic plastic zone size r_y and are equal in magnitude to the flow stress in compression ($-\sigma_o$) (Fig. 9a). By invoking Irwin's physically-adjusted crack length concept [49], we can envisage this situation as an equivalent elastic crack of length ($a + r_y$) with additional partial loading $\sigma_r = -\sigma_o$ at a distance *behind* the notional crack tip of $b \approx r_y$ (Fig. 9b). The stress intensity resulting from this partial loading K_{Ir} is given by [50] as

$$K_{Ir} = \frac{2\sqrt{2}}{\sqrt{\pi}} \sigma_r \sqrt{b} \quad , \tag{6}$$

for $b << 2H$ and a, the height of the specimen and the crack length respectively. For $\sigma_r = -\sigma_o$ and $b \approx r_y \sim 1/2\pi\,(\Delta K/2\sigma_o)^2$, the effective stress intensity range in the presence of the residual compressive stress field is given, by linear superposition, as

$$\Delta K_{eff} = K_{max} + K_{Ir} = K_{max} - \frac{\Delta K}{\pi} = K_{max}\left[1 - \frac{(1-R)}{\pi}\right], \quad \text{for } |K_{Ir}| \geq |K_{min}|,$$

$$\text{and} \quad = K_{max} - K_{min} = \Delta K, \qquad \text{for } |K_{Ir}| \leq |K_{min}|, \tag{7}$$

where R is the nominal load ratio. From Eq. (5), the critical load ratio,

above which (plasticity-induced) closure is ineffective, is thus where $K_{min} = K_{Ir}$ ($= \Delta K/\pi$), such that for a given ΔK at threshold

$$R_{cr} \simeq \frac{1}{1+\pi} \approx 0.24 \quad , \tag{8}$$

consistent with the experimentally observed result of $R_{cr} \simeq 0.3$ shown in Fig. 6 for a dry gaseous hydrogen environment where additional closure effects due to oxidation products are minimized.

Thus, the concept of (plasticity-induced) crack closure, the model of Paris and Schmidt [12] and our idealization based on residual compressive stresses is consistent with the present data shown in Fig. 6 of a constant $K_{o,max}$ at low R* and a constant ΔK_o at high R for threshold tests in gaseous environments, and with previously reported results for threshold behavior in low strength steels [12,23] and aluminum alloys [13]. However, it does not explain why behavior in the more oxidizing media of distilled water is distinctly different (Fig. 6), why thresholds (and the value of R_{cr}) are higher in moist air, nor why K_{cl} values are dependent upon the nature of the environment (Fig. 7). Furthermore, in view of the fact that near-threshold conditions are invariably in plane strain, it is unlikely that the observed effects of environment and load ratio can be explained solely based on plasticity-induced considerations.

---

*Based on this model for the contribution to plasticity-induced closure from residual stresses, with the assumption of a constant effective ΔK_{th} at threshold (12), Eq. (7) actually predicts a marginal decrease in $K_{o,max}$ with increasing R for $R < R_{cr}$[47], as shown by the threshold data for SA542-3 in Fig. 6 and for other steels in Refs. 23 and 47, for tests in dry environments.

IV.2 Oxide-Induced Crack Closure (OICC)

To account for the large closure effects reported for plane strain conditions in the near-threshold regime (see, for example, Ref. 35 and 51), several additional mechanisms of crack closure have recently been proposed [23-26,28-39, 41,42] based on the role of corrosion debris and fracture surface roughness in wedging the crack open at low stress intensities (Fig. 10). The first of these mechanisms, termed oxide-induced crack closure [23-25], arises from enlarged oxide deposits formed on freshly exposed surfaces at the crack tip in moist environments, which reach a thickness comparable to the crack tip opening displacements. As shown by the present results in SA542-3 steel (Fig. 4), the magnitude of such crack face oxide films can reach thicknesses up to ~ 0.7μm depending upon the growth rate, the load ratio and the nature of the environment. As discussed in detail elsewhere [23-26], the concept of oxide-induced crack closure has provided a very plausible explanation for the many effects of environment on near-threshold behavior, as shown in Fig. 3. In situations where the contributions to crack advance from "conventional" corrosion fatigue mechanisms (i.e. hydrogen embrittlement and active path corrosion) are minimal, i.e. for lower strength steels at the high frequencies ($\geq$50 Hz) commonly utilized for near-threshold measurements, the faster near-threshold growth rates (and lower thresholds) observed at low load ratios in dry hydrogen compared to moist air can be simply traced to a smaller contribution from oxide-induced crack closure arising from a lesser extent of crack face oxidation. The lower closure stress intensity K_{cl} values seen in dry hydrogen compared to moist air (Fig. 7) are clearly consistent with this inference. Furthermore, near-threshold growth rates have been observed, in low strength steels, to be similarly *faster* in dry helium gas [25], dehumidified oxygen [37] and dehumidified air [37], but to be relatively unchanged in moist hydrogen

[26] and water environments, when compared to moist air, again consistent with the concept of oxide-induced closure. However, in situations where "conventional" corrosion fatigue mechanisms are still active, as in the case of near-threshold tests on high strength steels [37,41, 52] and aluminum alloys [30,31] in moist environments, behavior is governed by a competition between two processes, namely hydrogen embrittlement or active path corrosion (which *increases* growth rates and *decreases* the threshold) and crack closure arising from the oxidation products (which *decreases* growth rates and *increases* the threshold).

Quantitatively, the significance of such crack face oxidation products in promoting closure where cyclic crack tip displacements are small, i.e., at near-threshold levels, can be estimated by considering the simple model of an idealized crack where the excess oxide layer is taken to be a rigid wedge of constant thickness d, extending along the crack length to a distance 2ℓ behind the crack tip (Fig.10). Assuming only a mechanical closure phenomenon arising from the excess material wedge within the crack and ignoring plasticity and hysteresis effects, calculations based on elastic superposition [50] using Barenblatt's singular integral equations [53] or the Westergaard stress function [54] yield a closure stress intensity value at the crack tip of:

$$K_{cl} = \frac{E'd}{4\sqrt{\pi\ell}} \quad , \tag{9}$$

where d can be taken as the maximum excess oxide thickness (d_o), 2ℓ the location behind the tip corresponding to the thickest oxide formation, and E' the plane strain elastic modulus [26]. Thus, by noting the equivalence between stress intensity and crack tip opening displacement (i.e. $\delta \approx K_I^2/2\sigma_o E'$), we can write for oxide-induced crack closure:

$$\left(\frac{K_{cl}}{K_{max}}\right)_{OICC} = \sqrt{\frac{d_o^2 C}{\pi \ell \delta_{max} \varepsilon_o}} \quad , \tag{10}$$

where ε_o is the yield strain (σ_o/E), δ_{max} the maximum crack tip opening displacement, and C is a constant of numerical value ~32^{-1}. Similar to Eq. (5), it again follows that, for a given ΔK at threshold, there will be a critical load ratio R_{cr} above which (oxide-induced) closure will be minimal, corresponding to the point when the minimum crack tip opening displacement δ_{min} exceeds d_o, i.e.

$$R = R_{cr} \text{ when } \delta_{min} \approx d_o, \text{ such that } R_{cr} \approx \sqrt{\frac{d_o}{\delta_{max}}} \quad . \tag{11}$$

Because of uncertainties associated with the location of the maximum oxide thickness, with the exact nature of contact between the crack faces, and with the oxide profile from the oxide peak to the crack tip, rigorous calculations of K_{cl} are clearly not feasible. However, by assigning reasonable values, some insight into the behavior depicted in Fig. 6 can be obtained. An estimate of 2ℓ can be obtained from scanning electron microscopy of fatigue samples, broken open in liquid nitrogen after cycling at threshold ΔK_o levels. From such fractographs (Fig. 11), the location of the oxide peak behind the crack tip (2ℓ) for SA542-3 steel tested in air (R = 0.05) was found to be of the order of 2 - 5μm.* With $\ell \approx$ 2μm, and a maximum oxide thickness (at ΔK_o) of $d_o \approx$ 0.2μm (Fig. 4), Eq. (9) yields a closure stress intensity at the threshold K_{cl} of the order of 4.5 MPa$\sqrt{m}$. For tests at R = 0.05 in dry hydrogen, where $d_o \approx$ 0.1μm, K_{cl} is estimated to be about 2.3 MPa$\sqrt{m}$, whereas at R = 0.75 in air or hydrogen, the value of K_{cl} is less than 0.25 MPa$\sqrt{m}$. Such estimates are clearly of the order of the experimentally measured values inferred from the ultrasonics results (Fig. 7), although it must be appreciated that there is a fair degree of uncertainty in both sets of values. However,

*Note because of a square root dependence of ℓ in Eq. (9), the exact numerical value becomes less critical.

taking these measured and predicted values, it is apparent that the difference in K_{cl} values at low R for moist air and dry hydrogen near-threshold conditions is of the order of 2 MPa$\sqrt{m}$, approximately equal to the difference in observed threshold ΔK_o values for the two environments.

Thus, in terms of the Paris and Schmidt model [12] for the role of load ratio (Fig.8), where now we assume contributions to closure to arise from both plasticity and oxide debris, it is to be expected that threshold ΔK_o values at low R will be lower in dry hydrogen gas since the extent of crack face oxidation (and hence oxide-induced crack closure) is considerably less than in moist air (Fig.6). Threshold ΔK_o values at high R, on the other hand, for these two environments would be expected to be similar since oxide thicknesses are similar and in this case comparable with their naturally-occurring oxide thicknesses (Table III), such that the role of closure is minimal. Furthermore, from Eq. (11) the value of R_{cr} would be expected to be higher in moist air since the overall level of oxidation is larger.

Threshold behavior in the more oxidizing medium of distilled water does not, at first sight, appear to fit with these ideas since the value of ΔK_o is far less dependent upon R (Fig 6). However, the extent of crack face oxidation is more uniform with respect to crack length (Figs. 4 and 5), and further the peak oxide thickness values (d_o) at the threshold are not decreased at high load ratios. This can be understood by considering the mechanisms of crack face oxide formation. In moist air and dry hydrogen, the naturally-occurring oxide films are small (~50-150 Å), and the size of the oxide debris formed on the crack surface at the threshold (d_o) at low R values is some 20-40 times thicker (Table III). A mechanism for this crack face oxide thickening in these environments can be envisaged in terms of "fretting oxidation" [55], i.e., a continual breaking and re-forming of the oxide scale behind the crack tip due to local heating and a

"smashing" together of the crack faces at low load ratios as a result of plasticity-induced crack closure aided by the strong Mode II crack tip displacements [56] characteristic of near-threshold crack advance. At high load ratios above R_{cr}, however, where closure effects are minimal and the Mode II displacements are considerably less pronounced [56], such fretting oxidation is insignificant and the extent of oxidation within the crack corresponds solely to that formed thermally, i.e., comparable with the natural oxide thickness (Table III). In more aggressive environments such as distilled water or steam, where the naturally-occurring oxide films are much thicker (~0.5-0.7μm), crack face oxide films can build up naturally to thicknesses comparable with the crack tip opening displacements without the need of fretting oxidation mechanisms. They therefore can remain uniformly thick at all load ratio levels (Fig. 6). Thus, in such oxidizing environments, a contribution from oxide-induced crack closure can persist even at high R values, and correspondingly the normally observed decrease in ΔK_o thresholds with increasing load ratio is much reduced. This explanation is consistent with threshold behavior reported for rotor steels tested in steam [42], where similarly the dependence of ΔK_o on R was less pronounced than in air.

IV.3 Roughness-Induced Crack Closure (RICC)

A third mechanism of crack closure which has relevance to the role of load ratio in influencing near-threshold fatigue crack growth is that induced by fracture surface roughness or morphology [25,33-38]. Such roughness-induced crack closure can arise where the size scale of the fracture surface roughness is comparable to crack tip opening displacements and where significant local Mode II displacements exist, such that the crack can become wedged open at discrete contact points along the crack faces (Fig. 10). This mechanism is most prevalent at near-threshold levels where maximum plastic zone sizes are typically less than the grain size [36,38,51]. In such instances, the low restraint on cyclic slip promotes crack

extension along a single slip system with combined Mode I and II displacements resulting in serrated or zig-zag fracture paths, which accentuate the closure effect. Recent studies [38] based on a geometric model for this phenomenon, have suggested that the extent of roughness-induced closure is primarily dependent upon the magnitude of the local Mode II crack tip displacements (u_{II}) and the roughness of the fracture surface (characterized in terms of the height h and the width w of the fracture surface asperites). In non-dimensional form, this analysis predicted that for roughness-induced closure [38]:

$$\left(\frac{K_{cl}}{K_{max}}\right)_{RICC} = \sqrt{\frac{2\gamma x}{1 + 2\gamma x}} \quad , \tag{12}$$

where x is the ratio of Mode II to Mode I displacements (u_{II}/u_I) and γ is a non-dimensional roughness factor equal to h/w. Limited experimental results for low and medium carbon steels were found to be consistent with Eq. (12) where the magnitude of the Mode II crack tip displacements was some 30 pct of the Mode I displacements [38]. Similar to the other modes of closure described above, for a given ΔK, there will again be a critical load ratio R_{cr} above which no closure due to surface roughness is possible. This will correspond to the point when the minimum crack tip opening displacement δ_{min} exceeds the scale of roughness h, i.e.

$$R = R_{cr}, \text{ when } \delta_{min} \approx h, \text{ such that } R_{cr} = \sqrt{\frac{h}{\delta_{max}}} \quad . \tag{13}$$

Quantitative estimates of the contribution to crack closure from this mechanism are experimentally complex since they involve an assessment of the magnitude of the local crack tip shear displacements [56]. Moreover, the relative dominance of this mechanism as opposed to the other plane strain closure phenomena is as yet not clearly understood. We include, however, a description of roughness-

induced crack closure simply because it represents an additional contribution to closure at near-threshold levels, which is likely to have particular significance to the load ratio effect in coarser-grained microstructures [36,38].

V. DISCUSSION

In agreement with numerous previous studies [1-26], it has been shown in this work that, for a lower strength pressure vessel steel, the influence of raising the load ratio R is in general to markedly increase near-threshold growth rates and to lower the threshold stress intensity range ΔK_o, below which crack growth apparently does not occur. The precise influence of load ratio, however, on such near-threshold behavior has been found to depend significantly upon the nature of the testing environment. Whereas the value of ΔK_o decreases quite sharply with increasing R for moist air and dry gaseous hydrogen environments (at least up to a critical load ratio R_{cr}), the load ratio dependence of ΔK_o in distilled water is found to be considerably less marked. Based on extensive measurements of crack face oxidation products, ultrasonic crack closure measurements and simple modelling studies, we attribute these effects of load ratio on near-threshold behavior primarily to the phenomenon of fatigue crack closure, although explanations based solely on Elber's well-known concept of plasticity-induced closure [2] are clearly inadequate to rationalize the variety of environmentally-influenced effects observed. Instead, we invoke additional mechanisms of closure, relevant to near-threshold (plane strain) conditions, which are promoted by the presence of rough, irregular fracture surfaces and particularly enlarged crack face oxidation products, such that the crack can become wedged-open at stress intensities above K_{min} (Fig. 10). Based the simple models for such plasticity-induced, roughness-induced and oxide-induced crack closure presented in this paper, it is clear that in all cases the general effect of increasing the load ratio is to lessen the influence of closure such that the

effective stress intensity range actually experienced at the crack tip is increased. However, since these closure mechanisms clearly act in concert, it is not feasible at this stage to quantitatively separate out the individual contributions from each mechanism. It is apparent, though, that plasticity-induced closure is enhanced by plane stress conditions [27], roughness-induced closure by coarse microstructures [36,38], and oxide-induced closure by oxidizing environments (as evidenced by behavior in distilled water), and that all mechanisms become less effective with increasing load ratio. In this regard, it is interesting that the marked microstructural and environmental effects commonly observed for near-threshold behavior at low load ratios (see Ref. 1, for example) are invariably far less apparent when tests are performed at high load ratios, again suggesting a prominent role of crack closure at near-threshold levels. However, it is worth noting here that the roughness and oxide-induced closure mechanisms are not necessarily uniquely confined to such ultralow growth rate regimes. Given a sufficient degree of faceted fracture morphology, such as is the case of "crystallographic" fatigue crack propagation in nickel-base superalloys [57], or substantial crack face oxidation, such as may occur for elevated temperature creep/fatigue crack growth [58], such mechanisms may be active at the larger crack tip displacements associated with cyclic crack advance at higher ΔK levels. Their effect, however, is maximized at near-threshold stress intensities due to the Mode I and Mode II character of the crack extension mechanisms there (akin to Forsyth's Stage I growth [59]) and from the small magnitude of the relative crack tip opening displacements.

Finally, the strong correlation between the load ratio dependence of threshold ΔK_o values and oxide-induced crack closure proposed in this paper may provide

an explanation for one of the more puzzling observations of near-threshold crack growth, namely that the effect of load ratio on ΔK_o for tests *in vacuo* has been generally observed to be slight [15,60], and in some cases almost non-existent [14,21]. Unlike behavior in moist air and dry hydrogen where a marked decrease in ΔK_o with increasing R follows from the fact that enlarged oxide deposits (formed by fretting oxidation mechanisms), and hence oxide-induced crack closure, are restricted to low load ratios only, behavior in the more oxidizing medium of water is characterized by a less pronounced decrease in ΔK_o with R because such enlarged deposits can form (by natural thermal oxidation processes) over the entire range of load ratios. In analagous fashion, it is not unreasonable to expect that where crack face oxidation is totally inhibited, i.e., for tests in high vacuum,* (oxide-induced) crack closure will again be largely independent of R and the resulting variation in ΔK_o with load ratio should be minimal. Such ideas await experimental verification.

---

*It should be noted that the analysis of near-threshold fatigue crack growth behavior *in vacuo* may be considerably more complex due to the possibility of crack face rewelding effects occurring during the fatigue cycle [1].

VI. CONCLUSIONS

Based on a study of the mechanisms for the load ratio dependence of fatigue crack propagation behavior, and specifically near-threshold behavior, in a lower strength 2-1/4Cr-1Mo pressure vessel steel tested at 50 Hz in moist air, dry gaseous hydrogen and distilled water environments, the following conclusions can be made:

1) Whereas variations in the load ratio had little influence on growth rates above ~10^{-6} mm/cycle, at lower, near-threshold levels the general effect of increasing the load ratio was to increase crack propagation rates and to decrease the threshold stress intensity range ΔK_o.

2) In moist air and dry gaseous (hydrogen) environments, threshold behavior was characterized at low load ratios by sharply decreasing ΔK_o values with increasing R (and a constant value of $K_{o,max}$) up to a critical load ratio R_{cr}. At higher load ratios above R_{cr}, the value of ΔK_o was constant in both environments and independent of R. The value of R_{cr} was found to be lower in the dry gaseous atmosphere.

3) In the more oxidizing medium of distilled water, threshold ΔK_o values were higher than in either moist air or dry hydrogen, particularly at high load ratios. In addition, the dependence of ΔK_o on R was far less pronounced.

4) Although scanning electron microscopy of near-threshold fracture surfaces revealed no significant changes in fracture morphology with either load ratio or environment, the extent of fracture surface oxidation products was found to be radically different. Using Auger spectroscopy, fracture surface oxide

films *at low load ratios*, in moist air and dry hydrogen environments, were found to be increased with decreasing stress intensity range to a peak value, near ΔK_o, some 20-40 times thicker than the limiting thickness of naturally formed oxide (~50-150 Å) for these environments, although the extent of crack-face oxidation was considerably less in the dry environments. Fracture surface oxide films *at high load ratios* (or at higher growth rates) were comparable in thickness with naturally formed oxide films.

5) In distilled water environments where the limiting thickness of naturally formed oxide layers is much higher (~0.5-0.7μm), fracture surface oxide films were found to be uniformly large *at all load ratios*.

6) Mechanistically, the load ratio dependence of threshold ΔK_o values and near-threshold growth rates is ascribed primarily to the phenomenon of crack closure. However, for the plane strain conditions of near-threshold behavior, the source of this closure is considered to arise not simply from Elber-type plasticity-induced crack closure but additionally from the effect of fracture surface morphology (roughness-induced closure) and principally from the presence of crack face oxide films (oxide-induced closure).

7) The difference in the load ratio-dependence of ΔK_o values for the environments tested is principally rationalized in terms of oxide-induced closure. In moist air and dry hydrogen environments where thick crack face oxides only form at low load ratios (by fretting oxidation), ΔK_o values decrease sharply with increasing R ($R<R_{cr}$). In distilled water, however, where oxides are uniformly thick at all load ratios, a contribution from oxide-induced closure can persist up to high load ratios such that the decrease in ΔK_o values with increasing R is far less pronounced.

8) Simple models are presented for plasticity-induced, roughness-induced and oxide-induced crack closure and are used to develop expressions for the

closure stress intensity K_{cl} and the critical load ratio value R_{cr}. Despite experimental uncertainties in the estimation of the extent of crack face oxidation, the fracture surface roughness and the interaction of the various closure mechanisms, the proposed expressions appear to be consistent with the load ratio-dependent near-threshold behavior observed.

9) Experimental measurements of closure stress intensities (K_{cl}) using ultrasonics techniques were found to confirm the proposition of an increased contribution from crack closure at low load ratios. Furthermore, values of K_{cl} were found to be lower in dry hydrogen compared to moist air, consistent with the concept of oxide-induced closure, and moreover to be numerically comparable to the model predictions.

ACKNOWLEDGMENTS

This work was supported by the Director, Office of Energy Research, Office of Basic Energy Sciences, Materials Science Division of the U. S. Department of Energy, under Contract No. DE-AC03-76SF00098. Thanks are due to Drs. J. D. Landes and D. M. McCabe of the Westinghouse Research and Development Center for supplying the steel.

NOMENCLATURE

a	crack length
b	distance behind notional crack tip over which residual stresses exist
C	constant ($\sim 32^{-1}$) in Eq. (10)
d	oxide thickness measured on fracture surface
d_o	maximum excess oxide thickness
da/dN	fatigue crack propagation rate per cycle
E'	elastic (Young's) modulus in plane strain
H	half height of specimen
h	height of fracture surface asperity
K_I	Mode I stress intensity factor
K_{Ir}	stress intensity due to residual compressive stress field
K_c	stress intensity at final failure (fracture toughness)
K_{cl}	stress intensity to cause closure of the crack
K_{max}	maximum stress intensity
K_{min}	minimum stress intensity
$K_{o,max}$	threshold maximum stress intensity for no crack growth
ΔK	alternating stress intensity ($K_{max} - K_{min}$)
ΔK_{eff}	effective stress intensity range ($K_{max} - K_{cl}$)
ΔK_o	threshold stress intensity range for no crack growth
ΔK_{th}	effective stress intensity range at the threshold for no crack growth
ℓ	half distance behind crack tip of maximum oxide thickness
N	number of cycles
R	load ratio (K_{min}/K_{max})
R_{cr}	critical load ratio above which crack closure cannot occur (at given ΔK)
r_y	cyclic plastic zone size ($\simeq 1/2\pi(\Delta K/2\sigma_o)^2$)
u_i	local crack tip displacements in Mode i = I,II
w	width of fracture surface asperity
x	ratio of Mode II to Mode I local crack tip displacements (u_{II}/u_I)
γ	non-dimensional fracture surface roughness factor (h/w)
ε_o	yield strain (σ_o/E')
δ	Mode I crack tip opening displacement (CTOD)
δ_{max}	maximum crack tip opening displacement at $K = K_{max}$
σ_{min}	minimum crack tip opening displacement at $K = K_{min}$
σ_o	yield strength
σ_r	residual compressive stress within cyclic plastic zone

REFERENCES

1. R. O. Ritchie, Int. Metals Rev., 20, 205 (1979).

2 W. Elber, in Damage Tolerance in Aircraft Structures, ASTM STP 486, p. 230 (1971).

3. L. P. Pook, in Stress Analysis and Growth of Cracks, ASTM STP 513, p. 106 (1972).

4. P. C. Paris, R. J. Bucci, E. T. Wessel, W. G. Clark, and T. R. Mager, ibid., p. 141.

5. R. J. Bucci, P. C. Paris, R. W. Hertzberg, R. A. Schmidt and A. F. Anderson, ibid., p. 125.

6. M. Klesnil and P. Lukâs, Eng. Fract. Mech., 4, 77 (1972).

7. R. J. Cooke and C. J. Beevers, Eng. Fract. Mech., 5, 1061 (1973).

8. R. O. Ritchie and J. F. Knott, Acta Metall., 21, 639 (1973).

9. R. O. Ritchie and J. F. Knott, Mater. Sci. Eng., 14, 7 (1974).

10. R. J. Cooke and C. J. Beevers, Mater. Sci. Eng., 13, 201 (1974).

11. J. Masounave and J.-P. Bailon, Scripta Metall., 9, 723 (1975).

12. R. A. Schmidt and P. C. Paris, in Progress in Flaw Growth and Fracture Toughness Tests, ASTM STP 536, p. 79 (1973).

13. A. Otsuka, K. Mori, and T. Miyata, Eng. Fract. Mech., 7, 429 (1975).

14. R. J. Cooke, P. E. Irving, G. S. Booth, and C. J. Beevers, Eng. Fract. Mech., 7, 69 (1975).

15. A. J. McEvily and J. Groeger, in Fracture 1977, (edited by D. M. R. Taplin), Univ. of Waterloo Press, Vol. 2, p. 1293 (1977).

16. C. Bathias, A. Pineau, J. Pluvinage, and R. Rabbe, ibid., p. 1283.

17. E. K. Priddle, ibid., p. 1249.

18. R. O. Ritchie, J. Eng. Mater. Technol.,(Trans. ASME, Ser. H), 99, 195 (1977).

19. R. O. Ritchie, Metall. Trans. A, 8A, 1131 (1977).

20. A. Ohta and E. Sasaki, Eng. Fract. Mech., 9, 307 (1977).

21. P. E. Irving and A. Kurzfeld, Met. Sci., 12, 495 (1978).

22. S. Suresh, C. M. Moss, and R. O. Ritchie, Trans. Japan Inst. Met., 21, 481 (1980).

23. R. O. Ritchie, S. Suresh, and C. M. Moss, J. Eng. Mater. Technol., (Trans. ASME, Ser. H), 102, 293 (1980).

24. A. T. Stewart, Eng. Fract. Mech., 13, 463 (1980).

25. S. Suresh, G. F. Zamiski, and R. O. Ritchie, Metall. Trans. A, 12A, 1435 (1981).

26. S. Suresh, D. M. Parks, and R. O. Ritchie, in Fatigue Thresholds, (edited by J. Bäcklund, A. F. Blom and C. J. Beevers), EMAS Ltd., Warley, U.K.(1982).

27. T. C. Lindley and C. E. Richards, Mater. Sci. Eng., 14, 281 (1974)

28. K. Endo, K. Komai, and Y. Matsuda, Memo Fac. Eng., Kyoto Univ., 31, 25 (1969).

29. H. Kitagawa, S. Toyohira, and K. Ikeda, in Fracture Mechanics in Engineering Applications, (edited by G. C. Sih and S. R. Valluri), Sijthoff and Noordhoff, The Netherlands, (1981).

30. S. Suresh, I. G. Palmer, and R. E. Lewis, Fat. Eng. Mat. Struct., (1982), in press.

31. A. K. Vasudevan and S. Suresh, Metall. Trans. A, to be published (1982).

32. P. K. Liaw, S. J. Hudak, and J. K. Donald, in Proc. of Fourteenth National Symposium on Fracture Mechanics, ASTM in press, Am. Soc. Test. Matls., Philadelphia, PA, (1982).

33. N. Walker and C. J. Beevers, Fat. Eng. Mat. Struct., 1, 135 (1979).

34. I. C. Mayes and T. J. Baker, Fat. Eng. Mat. Struct., 4, 79 (1981).

35. K. Minakawa and A. J. McEvily, Scripta Metall., 15, 633 (1981).

36. R. O. Ritchie and S. Suresh, Metall. Trans. A, 13A, (1982), in press.

37. R. O. Ritchie, in Fatigue Thresholds, (edited by J. Bäcklund, A. F. Blom, and C. J. Beevers), EMAS Ltd., Warley, U. K. (1982).

38. S. Suresh and R. O. Ritchie, Metall. Trans. A , to be published (1982).

39. S. Suresh and R. O. Ritchie, Met. Sci., 16, (1982), in press.

40. J. D. Frandsen, R. V. Inman, and O. Buck, Int. J. Fracture, 11, 345 (1975).

41. R. O. Ritchie, S. Suresh, and P. K. Liaw, in Fatigue and Corrosion Fatigue up to Ultrasonic Frequencies, (ed. by J. M. Wells and J. K. Tien), Eng. Foundation (1982).

42. B. L. Freeman, P. Smith, and A. T. Stewart, in Fatigue Thresholds (edited by J. Bäcklund, A. Blom, and C. J. Beevers)

43. V. Bachmann and D. Munz, Eng. Fract. Mech., 11, 61 (1979).

44. J. C. Newman, in Mechanics of Crack Growth, ASTM STP 590, p. 281 (1966).

45. J. Schijve, Delft University, Dept. of Aerospace Engineering, Memo No. M/336, Delft, The Netherlands (1979).

46. B. Budiansky and J. W. Hutchinson, J. Appl. Mech., (Trans. ASME, Ser. E), 45, 267 (1978).

47. S. Suresh and R. O. Ritchie, Scripta Metall., 16, (1982), to be published.

48. J. R. Rice, in Fatigue Crack Propagation, ASTM STP 415, p. 247 (1966).

49. G. R. Irwin, Appl. Mater. Res., 3, 65 (1964).

50. H. Tada, P. C. Paris, and G. R. Irwin, in Stress Analysis of Cracks Handbook, Del Corporation, Hellertown, PA (1973).

51. R. J. Asaro, L. Hermann and J. M. Baik, Metall. Trans. A, 12A, 1135 (1981).

52. J. Toplosky and R. O. Ritchie, Scripta Metall., 15, 905 (1981).

53. G. I. Barenblatt, in Advances in Applied Mechanics, Academic Press, New York, vol. 7, p. 55 (1962).

54. H. M. Westergaard, J. Appl. Mech., (Trans. ASME, Ser. A), 66, 49 (1939).

55. D. Benoit, R. Namdar-Tixier, and R. Tixier, Mater. Sci. Eng., 45, 1 (1981).

56. D. L. Davidson, Fat. Eng. Mat. Struct., 3, 229 (1981).

57. M. Gell and G. R. Leverant, Acta Metall., 16, 553 (1968).

58. R. P. Skelton and J. R. Haigh, Mater. Sci. Eng., 3, 17 (1978).

59. P. J. E. Forsyth, in Crack Propagation, Proc. Symp., Cranfield College of Aeronautics, p. 76, Cranfield Press, (1962).

60. T. C. Lindley and C. E. Richards, Central Electricity Generating Board Note No. RD/L/N 135/78, CERL, U.K., (1978).

Table I. Base Plate Chemistry of SA542-3 (Wt. Pct.)

C	Mn	Si	Ni	Cr	Mo	P	S	Cu
0.12	0.45	0.21	0.11	2.28	1.05	0.014	0.015	0.12

Table II. Room Temperature Mechanical Properties of SA542-3

0.2% Offset Yield Strength		U.T.S.	Redn. in Area	K_{Ic}	$K_{Iscc}(H_2 gas)$
monotonic (MPa)	cyclic (MPa)	(MPa)	(Pct)	(MPa$\sqrt{m}$)	(MPa$\sqrt{m}$)
500	400	610	77	295	85

Table III. Room Temperature Oxide Thickness Data for SA542-3 Steel, Under Naturally Exposed and Near-Threshold Fatigue Conditions

Environment	Load Ratio (K_{min}/K_{max})	Naturally-Occurring Oxide Thickness (μm)	Peak Crack Face Oxide Thickness (d_o) at ΔK_o (μm)
Moist Air	0.05	0.01 ± 0.005	0.20 ± 0.050
	0.75	0.01 ± 0.005	0.01 ± 0.005
Dry Hydrogen	0.05	0.01 ± 0.005	0.09 ± 0.040
	0.75	0.01 ± 0.005	0.01 ± 0.005
Distilled Water	0.05	0.60 ± 0.100	0.55 ± 0.100
	0.75	0.60 ± 0.100	0.70 ± 0.200

LIST OF FIGURE CAPTIONS

Fig. 1: Experimental set-up for the measurement of crack closure using ultrasonics techniques.

Fig. 2: Variation in fatigue crack propagation rates (da/dN) with alternating stress intensity (ΔK) for bainitic 2-1/4Cr-1Mo steel (SA542-3) tested in ambient temperature moist air over a range of load ratios from R = 0.05 to 0.75.

Fig. 3: Influence of environment on near-threshold fatigue crack growth in SA542-3 tested at R = 0.05 and 0.75. Room temperature moist air data from Fig. 2 are compared with data for wet and dry gaseous hydrogen and distilled water environments.

Fig. 4: Measurements of crack face oxide thickness as a function of crack length (a) and crack growth rate (da/dN) for SA542-3 steel tested in moist air, dry gaseous hydrogen and distilled water at R = 0.05 and 0.75. Data from Ar^+ sputtering analysis using Auger spectroscopy.

Fig. 5: Visual observations of corrosion deposits on near-threshold fatigue fracture surfaces of SA542-3 tested in a) moist air at R = 0.05, b) moist air at R = 0.75, and c) distilled water at R = 0.75.

Fig. 6: Variation of alternating and maximum stress intensities at threshold (ΔK_o and $K_{o,max}$ respectively) and the maximum excess oxide thickness (d_o) with load ratio R for SA542-3 steel tested in ambient temperature environments of moist air, dry gaseous hydrogen and distilled water at 50 Hz.

Fig. 7: Crack closure measurements at ΔK_o using ultrasonics technique in terms of the variation of ultrasonic receiver signal with load and stress intensity in SA542-3 steel, showing how near-threshold cracks open and close in moist air and dry gaseous hydrogen at R = 0.05 and 0.50.

Fig. 8: Load ratio model of Paris and Schmidt showing their expected variation in threshold stress intensity values, ΔK_o and $K_{o,max}$, with load ratio R (after Ref. 12).

Fig. 9: Schematic illustrations of the plastic zones ahead of a fatigue crack where the effect of the residual compressive stress field ($\sigma_r = -\sigma_o$) within the cyclic plastic zone (r_y) is modelled as an equivalent crack of length $a + r_y$, partially loaded behind the notional crack tip over a distance $b \approx r_y$.

Fig. 10: Summary of the various mechanisms of fatigue crack closure with their respective analytical expressions.

Fig. 11: Showing the region of maximum oxide thickness (blurred region) a short distance (2ℓ) behind the crack tip at the threshold. Specimen of SA542-3 steel cycled at ΔK_o in moist air at R = 0.05, and then broken open in liquid nitrogen. Region A shows near-threshold fatigue, B final failure by cleavage, and O the approximate area of maximum oxide thickness. Arrows indicate position of fatigue crack front.

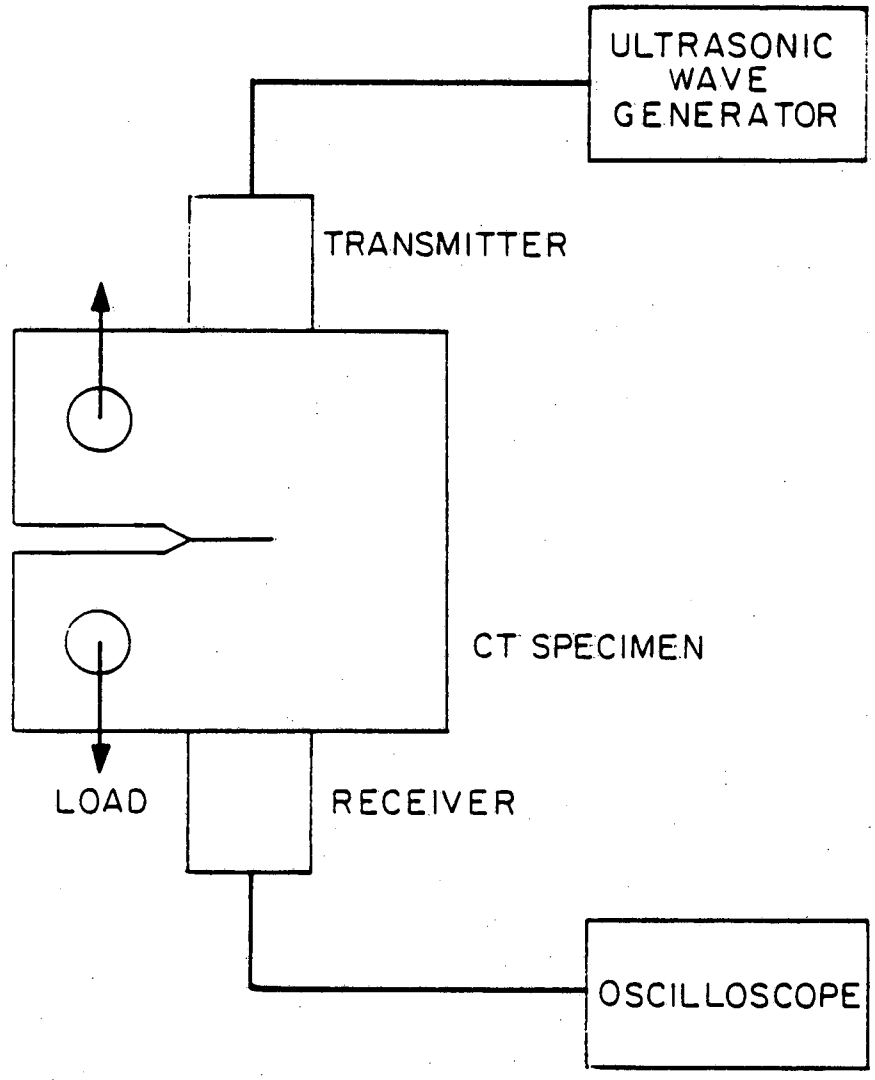

XBL 824-9314

Fig. 1: Experimental set-up for the measurement of crack closure using ultrasonics techniques.

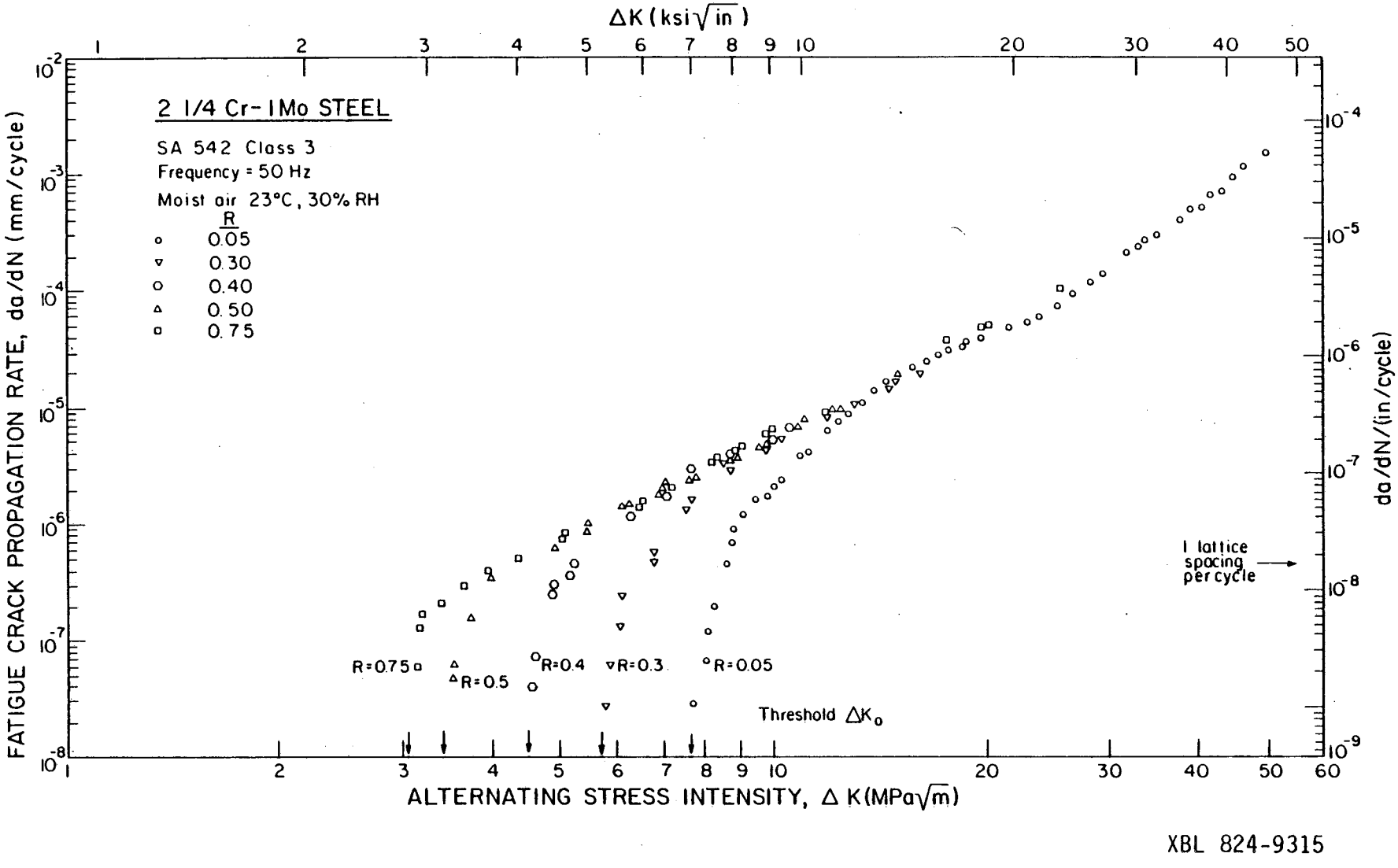

Fig. 2: Variation in fatigue crack propagation rates (da/dN) with alternating stress intensity (ΔK) for bainitic 2-1/4Cr-1Mo steel (SA542-3) tested in ambient temperature moist air over a range of load ratios from R = 0.05 to 0.75.

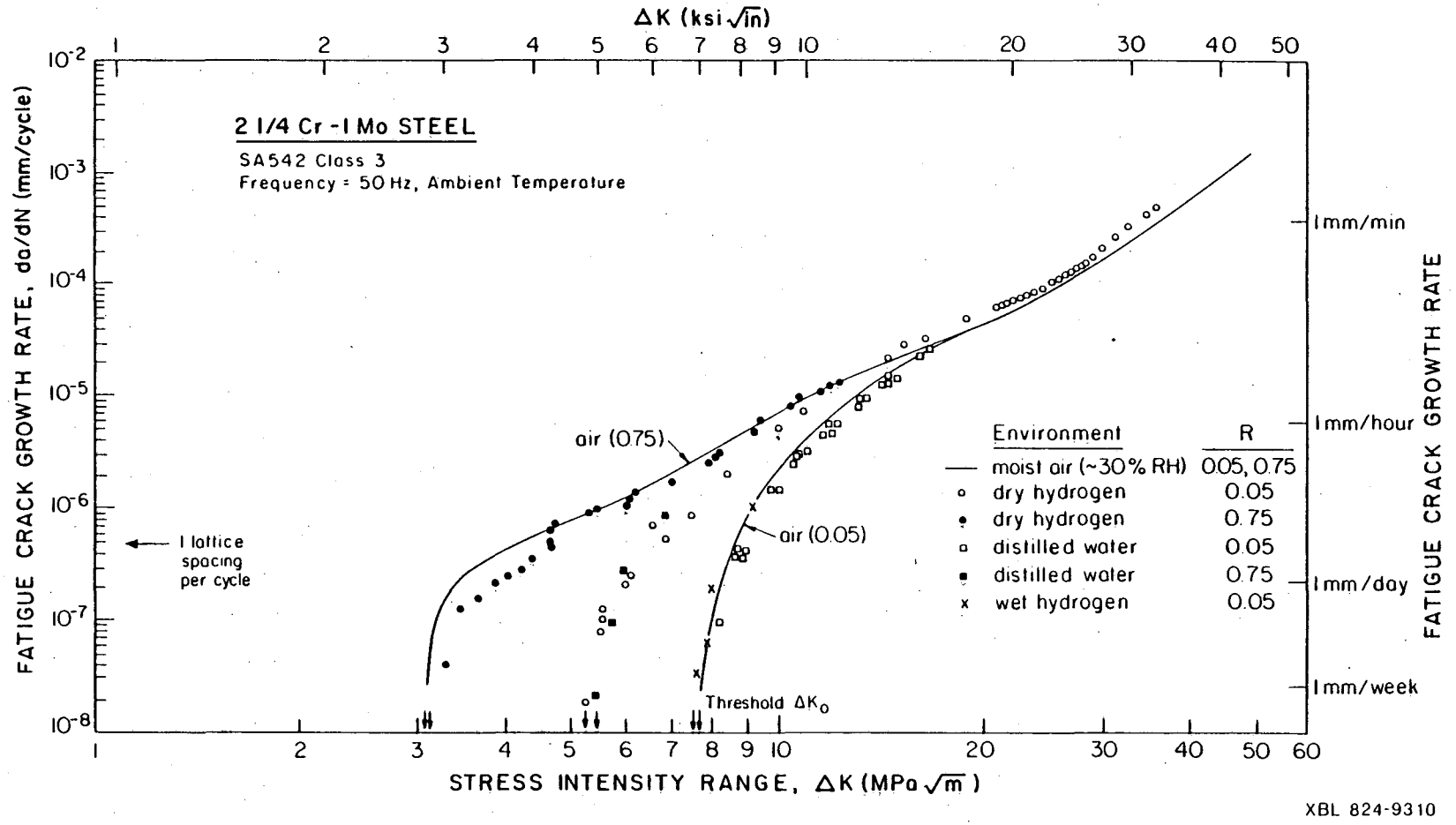

Fig. 3: Influence of environment on near-threshold fatigue crack growth in SA542-3 tested at R = 0.05 and 0.75. Room temperature moist air data from Fig. 2 are compared with data for wet and dry gaseous hydrogen and distilled water environments.

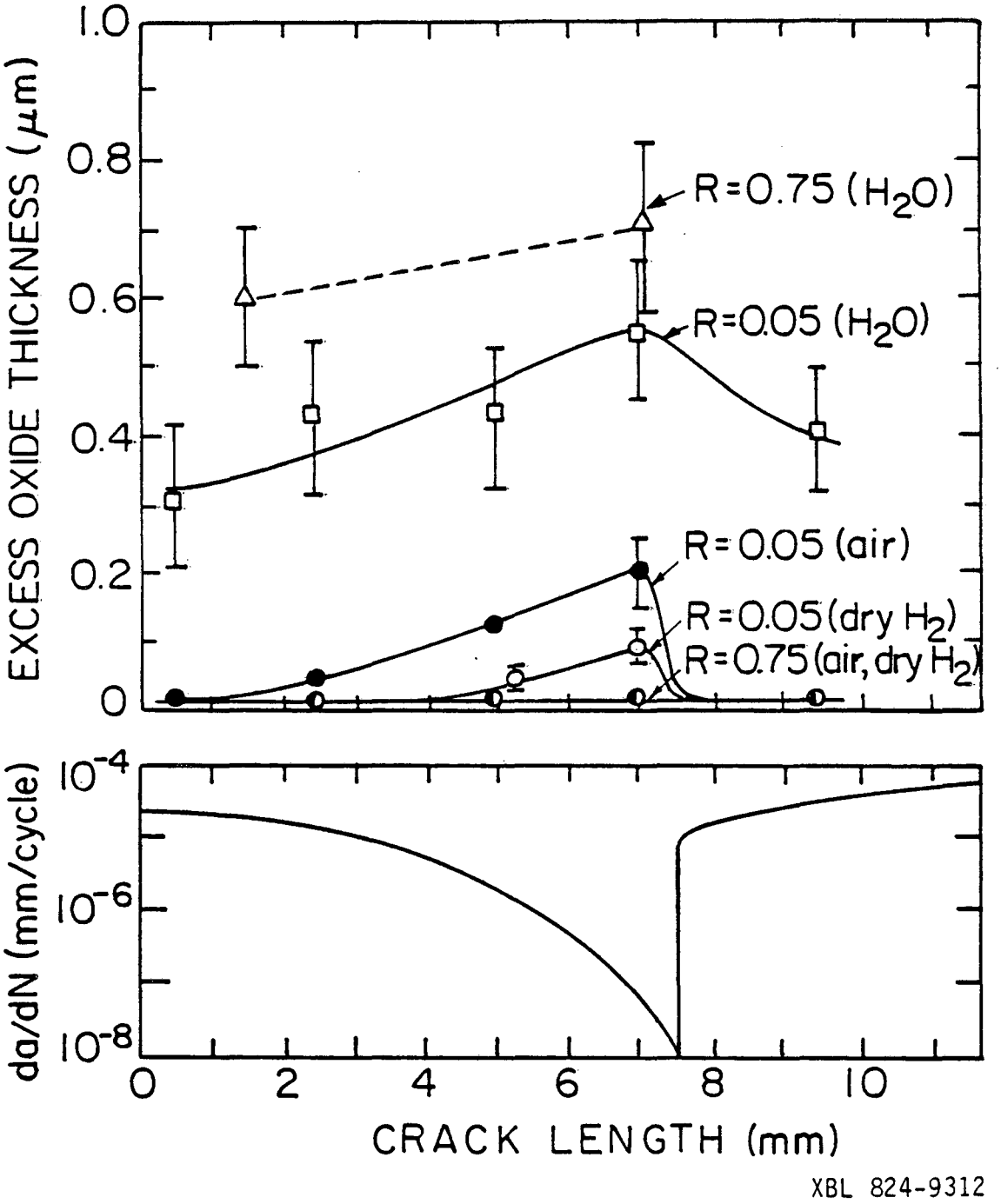

Fig. 4: Measurements of crack face oxide thickness as a function of crack length (a) and crack growth rate (da/dN) for SA542-3 steel tested in moist air, dry gaseous hydrogen and distilled water at R = 0.05 and 0.75. Data from Ar^+ sputtering analysis using Auger spectroscopy.

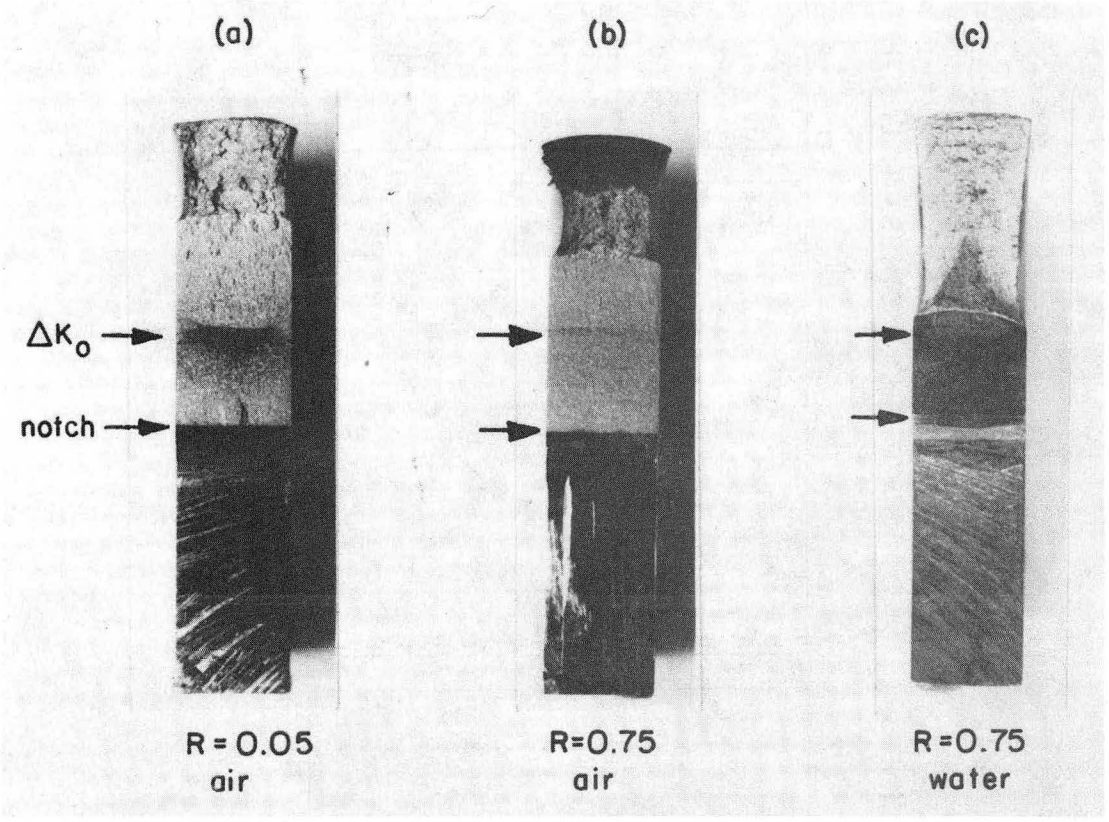

XBB 824-3696

Fig. 5: Visual observations of corrosion deposits on near-threshold fatigue fracture surfaces of SA542-3 tested in a) moist air at R = 0.05, b) moist air at R = 0.75, and c) distilled water at R = 0.75.

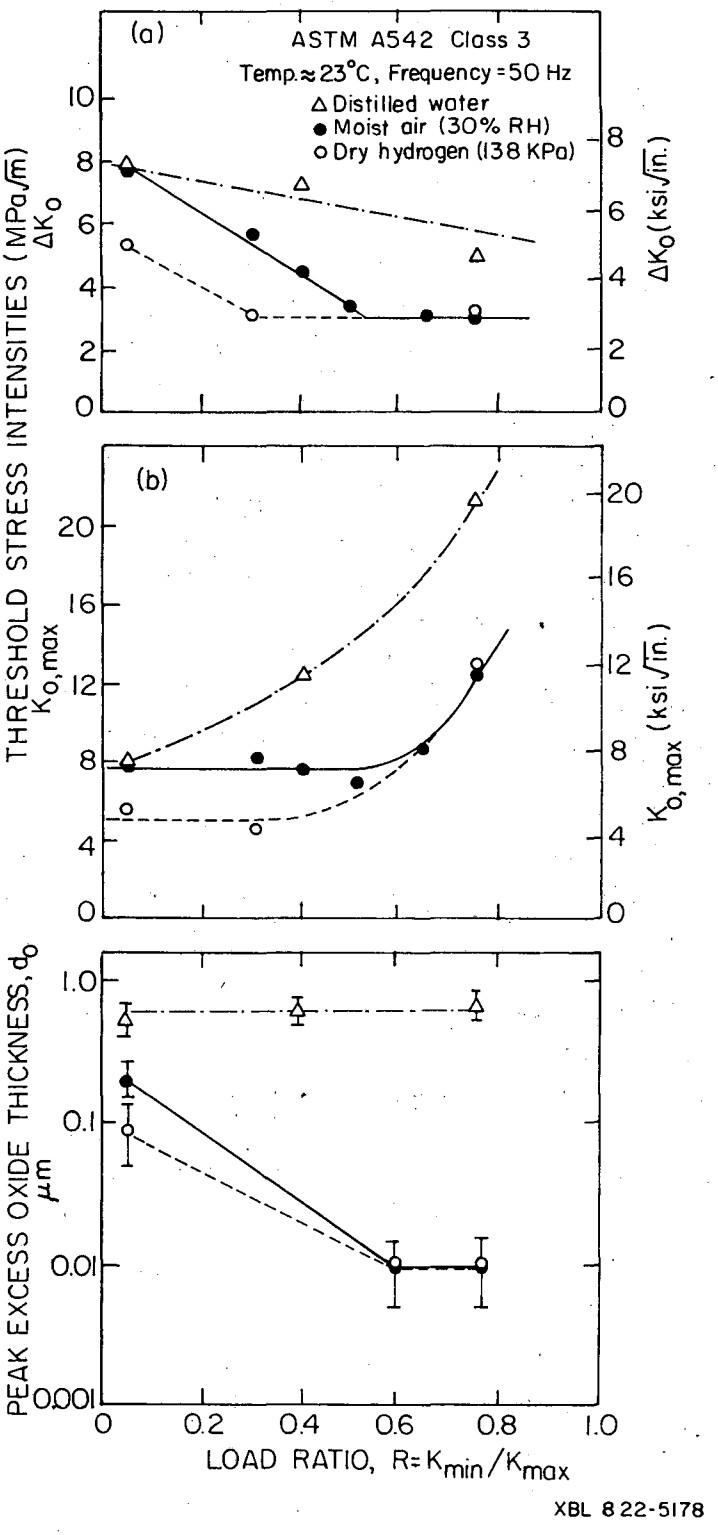

Fig. 6: Variation of alternating and maximum stress intensities at threshold (ΔK_o and $K_{o,max}$ respectively) and the maximum excess oxide thickness (d_o) with load ratio R for SA542-3 steel tested in ambient temperature environments of moist air, dry gaseous hydrogen and distilled water at 50 Hz.

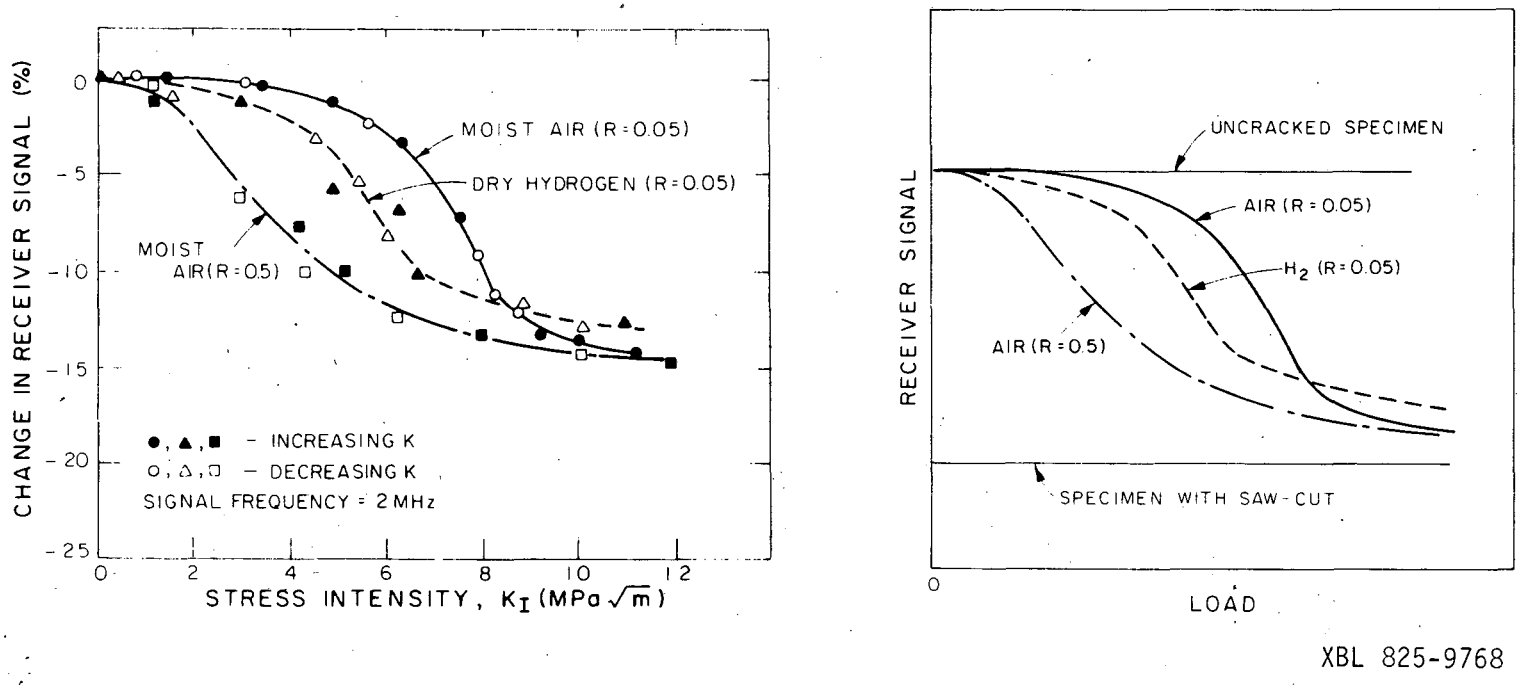

XBL 825-9768

Fig. 7: Crack closure measurements at ΔK_0 using ultrasonics technique in terms of the variation of ultrasonic receiver signal with load and stress intensity in SA542-3 steel, showing how near-threshold cracks open and close in moist air and dry gaseous hydrogen at R = 0.05 and 0.50.

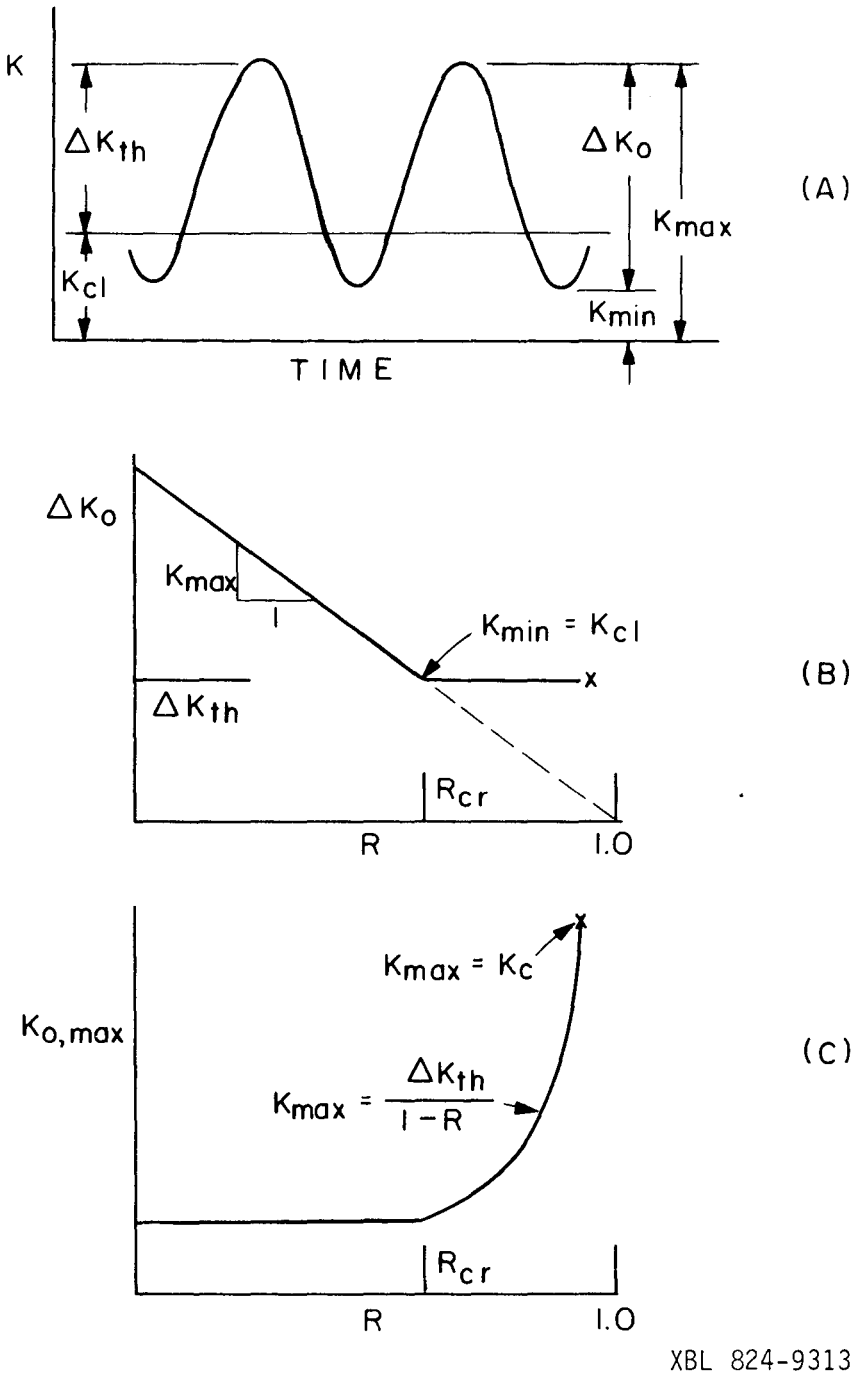

Fig. 8: Load ratio model of Paris and Schmidt showing their expected variation in threshold stress intensity values, ΔK_o and $K_{o,max}$ with load ratio R (after Ref. 12).

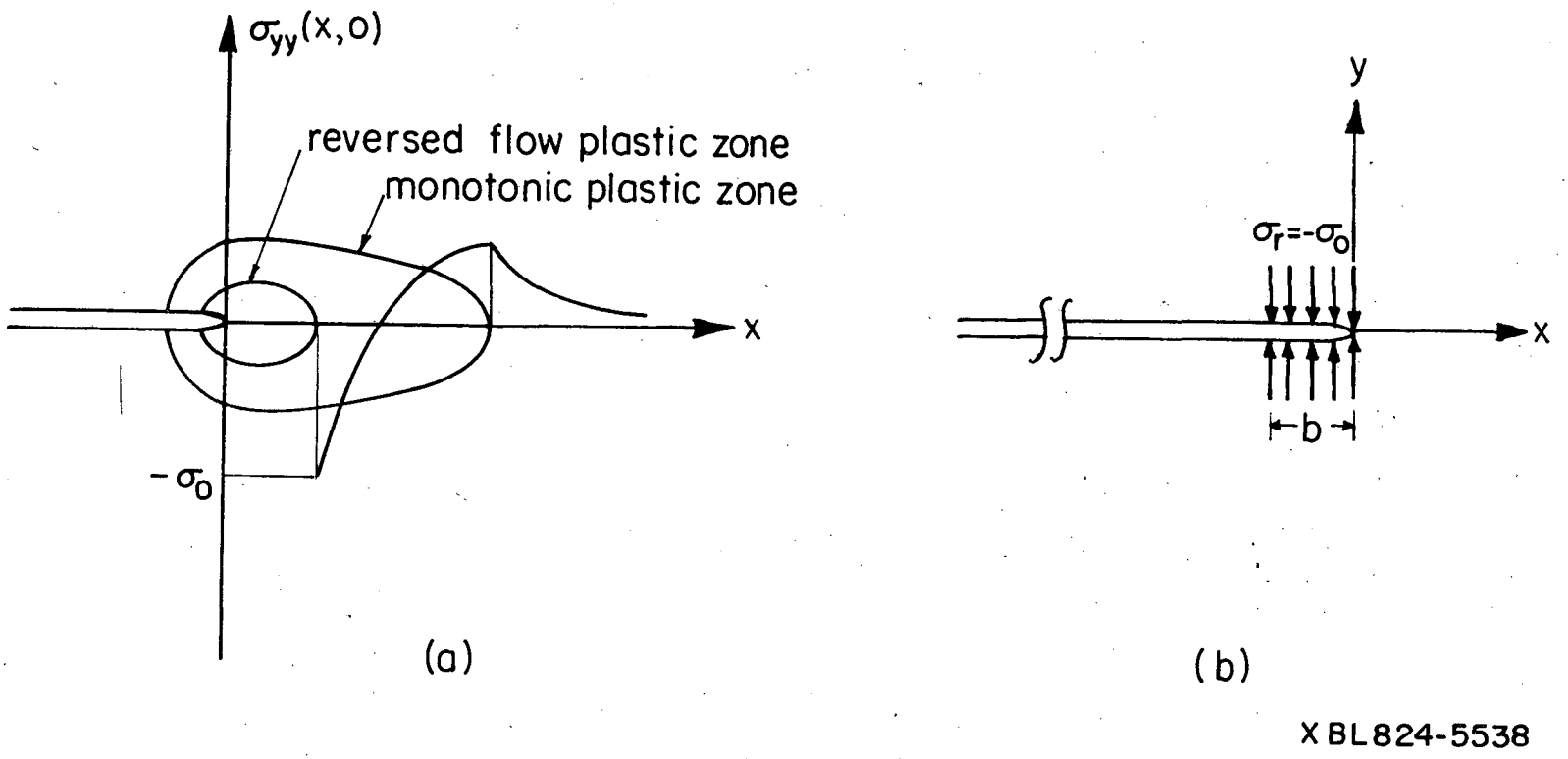

Fig. 9: Schematic illustrations of the plastic zones ahead of the fatigue crack where the effect of the residual compressive stress field ($\sigma_r = -\sigma_o$) within the cyclic plastic zone (r_y) is modelled as an equivalent crack of length $a + r_y$, partially loaded behind the notional crack tip over a distance $b \approx r_y$.

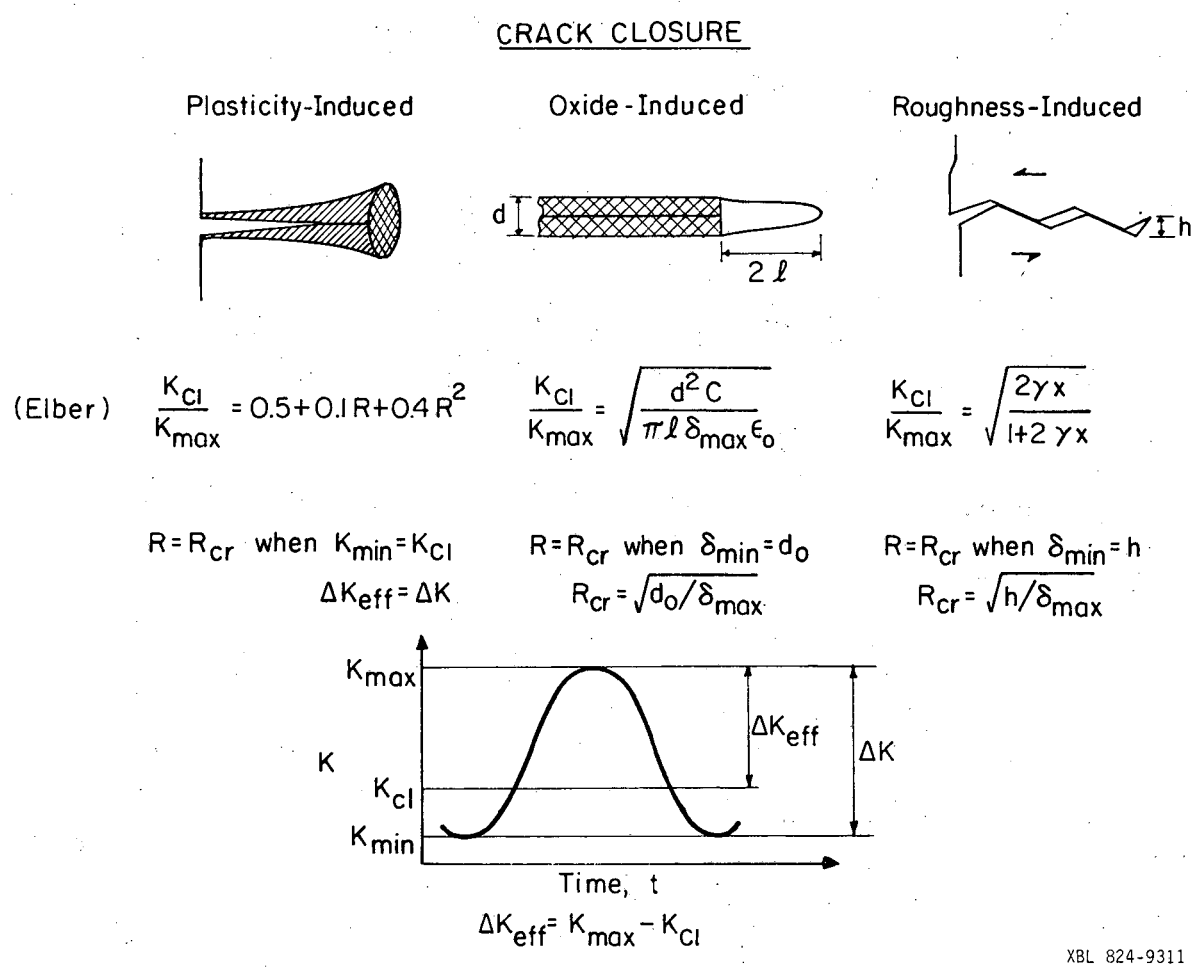

Fig. 10: Summary of the various mechanisms of fatigue crack closure with their respective analytical expressions.

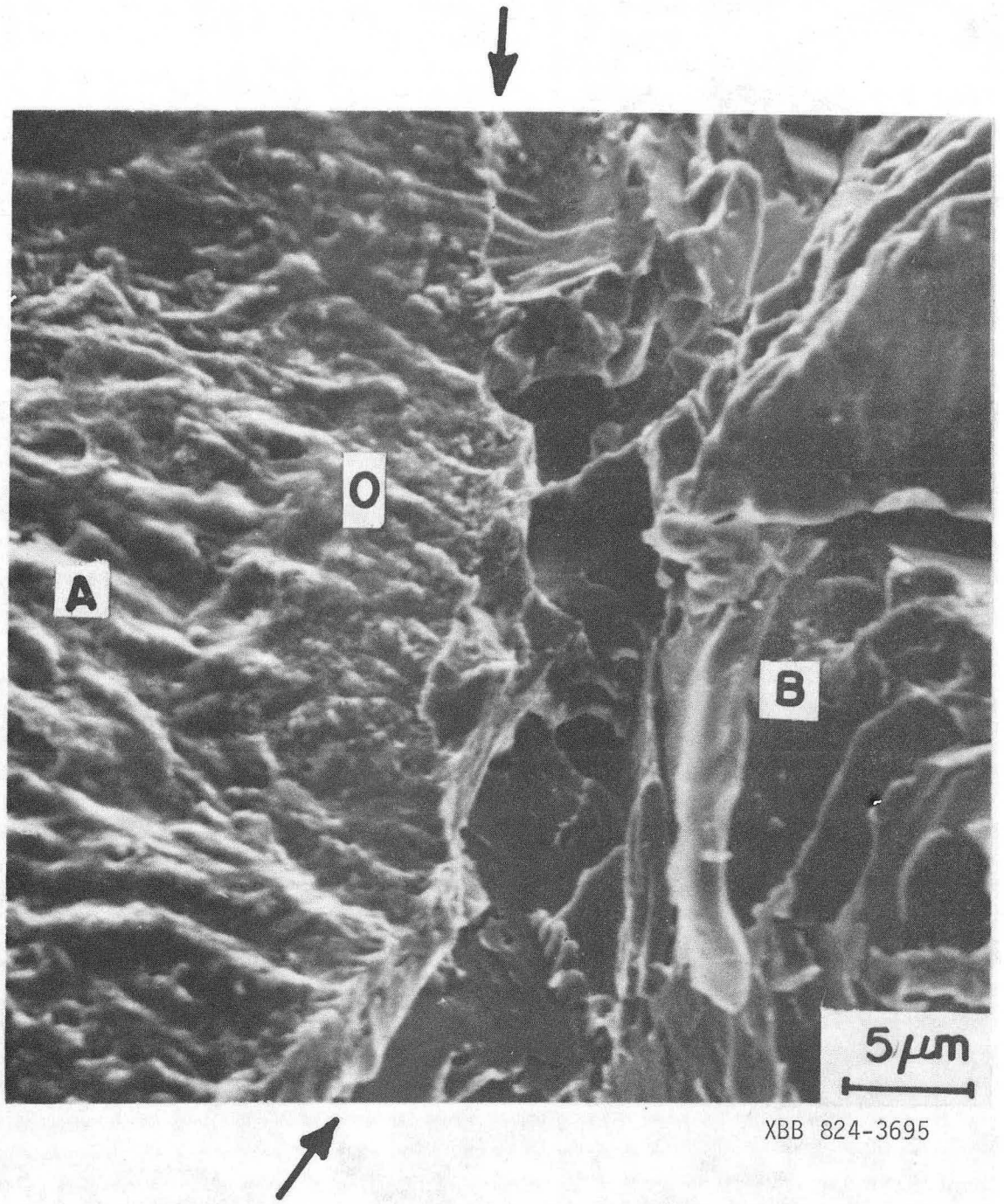

Fig. 11: Showing the region of maximum oxide thickness (blurred region) a short distance (2ℓ) behind the crack tip at the threshold. Specimen of SA542-3 steel cycled at ΔK_0 in moist air at R = 0.05, and then broken open in liquid nitrogen. Region A shows near-threshold fatigue, B final failure by cleavage, and O the approximate area of maximum oxide thickness. Arrows indicate position of fatigue crack front.

TECHNICAL INFORMATION DEPARTMENT
LAWRENCE BERKELEY LABORATORY
UNIVERSITY OF CALIFORNIA
BERKELEY, CALIFORNIA 94720